frontiers | Frontiers in Marine Science

TYPE Original Research
PUBLISHED 24 March 2023
DOI 10.3389/fmars.2023.1147292

OPEN ACCESS

EDITED BY
Yeping Yuan,
Zhejiang University, China

REVIEWED BY
Yongxiang Huang,
Xiamen University, China
Shuang-Xi Guo,
South China Sea Institute of Oceanology (CAS), China

*CORRESPONDENCE
Huan Mei
hmei@just.edu.cn
Qian Liu
liuqian@just.edu.cn

SPECIALTY SECTION
This article was submitted to Physical Oceanography, a section of the journal Frontiers in Marine Science

RECEIVED 18 January 2023
ACCEPTED 10 March 2023
PUBLISHED 24 March 2023

CITATION
Li K, Mei H, Wu X, Dong J and Liu Q (2023) Influence of multiple islands on the hysteresis and dynamics of a western boundary current perturbed by a mesoscale eddy at a gap.
Front. Mar. Sci. 10:1147292.
doi: 10.3389/fmars.2023.1147292

Influence of multiple islands on the hysteresis and dynamics of a western boundary current perturbed by a mesoscale eddy at a gap

Kunshan Li, Huan Mei*, Xiangbai Wu, Jianxin Dong and Qian Liu*

School of Naval Architecture and Ocean Engineering, Jiangsu University of Science and Technology, Zhenjiang, China

The hysteresis of a western boundary current (WBC) flowing across a gap and the dynamics of the mesoscale eddy–WBC interaction with the presence of two islands in the gap are studied using a 1.5-layer ocean model. The hysteresis of the WBC suggests that the two islands in the gap facilitate the WBC to intrude into the western basin by shedding eddies compared with the no-island case, but they promote the WBC to leap across the gap compared with the one-island case. The mesoscale eddies from the east of the gap can induce the critical-state WBC shifting from penetration to leap and vice versa. The dynamics revealed by the vorticity balance analysis shows that the increased (decreased) meridional advection of the WBC perturbed by the eddy forces the WBC to leap across (intrude into the western basin through) the gap. We also present the parameter space of the critical strength of the eddy with variable north–south locations inducing the critical WBC transition. For the WBC critical from the eddy-shedding to leaping regime, the regime shift is most sensitive to the anticyclonic eddy from the gap center and to the cyclonic eddy from the southern gap. It is least sensitive to the eddy downstream of the WBC. For the WBC critical from the leaping to eddy-shedding regime, the regime shift is most sensitive to the anticyclonic eddy upstream of the WBC and to the cyclonic eddy from the southern gap. The least sensitive eddy is from the northern gap.

KEYWORDS

South China Sea, mesoscale eddy, western boundary current, dynamics, island

1 Introduction

The South China Sea (SCS) is a semi-enclosed marginal sea in the northwestern Pacific Ocean and extends from the equator to 23°N and from 99° to 121°E. The SCS connects the Indian Ocean through the Malacca Strait and the Northwest Pacific Ocean through the Luzon Strait. The Luzon Strait is a wide gap between Taiwan of China and Luzon of

the Philippines, with a meridional width of ~340 km and a maximum depth of more than 2,500 m. The Luzon Strait is the most important channel of mass, momentum, and energy exchanges between the SCS and the Pacific Ocean (Nitani, 1972; Qu et al., 2000; Qu et al., 2004; Caruso et al., 2006; Nan et al., 2015; Shen et al., 2022). The Kuroshio, a strong western boundary current (WBC) in the northwestern Pacific, originates from the northern branch of the North Equatorial Current east of Luzon Island and flows northward along the eastern Philippine coast. The Kuroshio either intrudes into the SCS through the gap or leaps across the gap as it passes by the Luzon Strait (treated as a gap in this study) (Nitani, 1972; Yuan et al., 2006; Song et al., 2018; Song et al., 2019; Yuan et al., 2019). The Kuroshio intrusion has been confirmed to exhibit different intruding paths southwest of Taiwan (Metzger and Hurlburt, 2001; Sheremet, 2001; Caruso et al., 2006; Yuan et al., 2006; Sheremet and Kuehl, 2007; Kuehl & Sheremet, 2009). Caruso et al. (2006) identified five types of Kuroshio paths, including the Kuroshio SCS branch, the Kuroshio loop, the detached anticyclonic eddy, the cyclonic intrusion, and the leaping path. The integral of geostrophic vorticity was also used to identify three typical Kuroshio paths: the looping path, the leaking path, and the leaping path (Nan et al., 2011; Nan et al., 2015). The hysteresis is considered to be one of the most important dynamic mechanisms to explain the Kuroshio intrusion. Sheremet (2001) studied the hysteresis of a WBC using a quasi-geostrophic model and summarized the gap-leaping problem in the balance between the beta effect (promoting the penetration) and the inertia (promoting the leap). Next, the presence of the multiple states and hysteresis of the WBC in a gap-leaping system was verified in laboratory experiments (Sheremet and Kuehl, 2007; Kuehl and Sheremet, 2009; Kuehl and Sheremet, 2014; McMahon et al., 2021). Moreover, the external factors, i.e., meridional wind (Wang et al., 2010), island in the gap (Mei et al., 2019), mesoscale eddy (Yuan and Li, 2008; Yuan and Wang, 2011; Mei et al., 2022), and large-scale circulation in the SCS (Mei et al., 2023), are also proved to be crucial to affect the WBC path in a gap-leaping system. As for the other aspects, Wang and Yuan (2012); Wang and Yuan (2014) studied the collision of two opposite WBCs with equal or unequal transport at a gap, and Song et al. (2019) and McMahon et al. (2021) studied the effect of throughflow on the WBC transition. In addition to the Kuroshio, the Gulf of Mexico Loop Current is another example of the application of hysteresis and multiple equilibrium states of the WBC to the gap-leaping problem (Kuehl and Sheremet, 2022; Sheremet et al., 2022).

In the vicinity of the Luzon Strait, the westward-moving mesoscale eddies from the northwestern Pacific interact with the WBC and frequently induce the variation of the WBC path (Yuan et al., 2006; Yuan and Li, 2008; Sheu et al., 2010; Yuan and Wang, 2011; Zhong et al., 2016; Yang et al., 2020; Mei et al., 2022). A reduced-gravity model was used to study the interaction of an eddy with a WBC by Chern and Wang (2005) and Kuo and Chern (2011); however, a gappy western boundary was not considered in their idealized model. In a gap-leaping system, on the one hand, the interactions of a mesoscale eddy with a WBC far away from the critical state and a critical-state WBC in the vicinity of the gap were studied by Song et al. (2018) and Yuan et al. (2019), respectively. They focused on the evolution and development of the eddy rather than those of the WBC transition. On the other hand, Yuan and Wang (2011) focused on the WBC transition perturbed by a mesoscale eddy in a gap-leaping system and found that both cyclonic and anticyclonic eddies could induce the critical-state WBC shifting regimes from penetration to leap, while only cyclonic eddies could induce the WBC transition from leap to penetration. Mei et al. (2022) considered the effect of an island with variable meridional sizes on the eddy–WBC interaction. They found that both anticyclonic and cyclonic eddies could shift regimes of the critical-state WBC from penetration to leap, and vice versa. Figure 1 shows a Kuroshio Loop current eddy-shedding event using the AVISO altimeter data (http://www.aviso.oceanobs.com/). The Kuroshio leaped across the Luzon Strait initially (Figures 1A, B). Meanwhile, an anticyclonic eddy from the northwestern Pacific moved westward to impinge and interact with the Kuroshio near the southeastern location of the Luzon Strait, and then it moved northward along with the Kuroshio. As the eddy interacted fully with the Kuroshio, a loop current was gradually formed in the vicinity of the Luzon Strait (Figure 1C). Lastly, an anticyclonic eddy was shed from the Kuroshio, and the main stream of the Kuroshio leaped across the gap again (Figure 1D). In this case, it seems that the perturbation of the eddy from the east induces the Kuroshio transition between penetration and leap and will be explored in this study.

In fact, there are two island chains in the Luzon Strait, including the southern Babuyan Island chain composed of the Camiguin, Calayan, Fuga, and Dalupiri Islands, and the central Batanes Island chain composed of the Sabtang, Batanes, and Itbayat Islands, as shown in Figure 1 (Liang et al., 2008; Huang et al., 2017). Intuitively, these island chains may influence the WBC intrusion into the SCS to some extent. Metzger and Hurlburt (2001) found that the Calayan Bank and a shoal north of the Calayan Island within the Luzon Strait reduce the westward intrusion of the Kuroshio into the SCS by using the NRE Layered Ocean Model. Mei et al. (2019); Mei et al. (2022) investigated the influence of an island on the WBC regime and found that the presence of an island promotes the WBC shedding eddies compared with the no-island case in the gap. Previous numerical studies focus on the effect of one island in the gap (resembling the central Batanes Island), which facilitates the WBC intrusion usually. However, the southern Babuyan Island may conversely prevent the Kuroshio from intruding into the SCS to some extent because the WBC leaps across the gap more easily as the southern gap width decreases, as examined by Mei et al. (2019). To what extent the combined quantitative impacts the southern and central islands on the WBC hysteresis and the critical-state WBC transition is worth studying. This paper is a continuation of Mei et al. (2019); Mei et al. (2022) and further considers the eddy–WBC interaction in the vicinity of a gap between two islands, which resemble the central Batanes Island and the southern Babuyan Island in the Luzon Strait.

In this study, we use a non-linear 1.5-layer ocean model to study the hysteresis of the WBC with two islands in the gap and the dynamics of the critical-state WBC transition impinged by a mesoscale eddy from the east. The model is described in Section 2. The hysteresis of the WBC with two islands in the gap and the

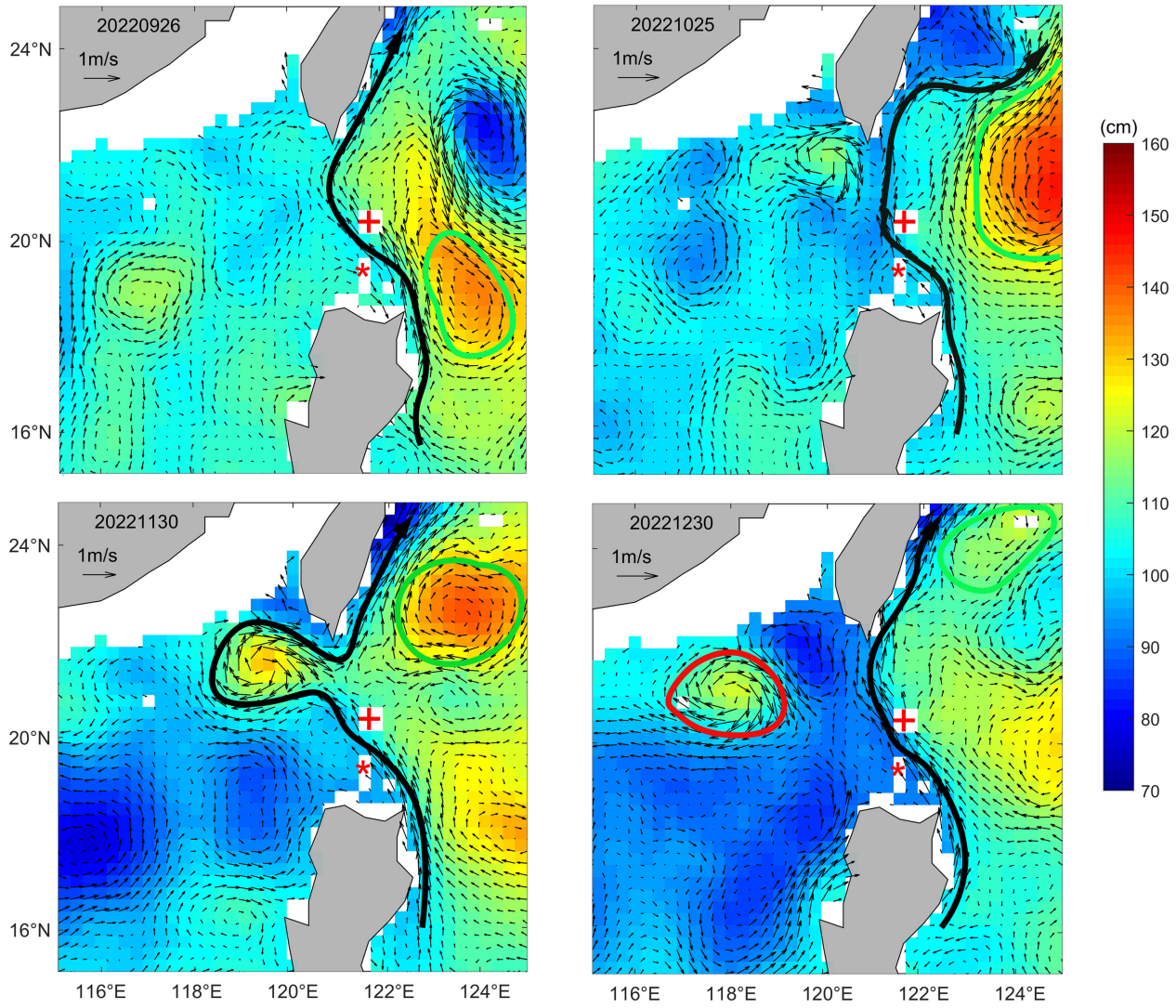

FIGURE 1
Absolute dynamical topography (cm; shading) and geostrophic currents (m/s; vector) in the northeastern SCS showing an anticyclonic eddy shed from the Kuroshio in 2022. A westward-moving anticyclonic eddy from the northwestern Pacific interacted with the Kuroshio in the Luzon Strait area inducing the Kuroshio transition. Regions with water shallower than 100 m are in white. The Batanes Island Chain and Babuyan Island Chain are marked by red plus and asterisk, respectively. The black, red, and green bold curves represent the Kuroshio axis, the anticyclonic eddy shed from the Kuroshio, and the westward-moving anticyclonic eddy from the northwestern Pacific, respectively. SCS, South China Sea.

dynamics of the eddy–WBC interaction are studied in Section 3. The conclusion and discussion are given in Section 4.

2 The model

In this study, a non-linear 1.5-layer reduced gravity model is adopted for simulation. The application of the model to the western Pacific Ocean, the Luzon Strait, and the SCS has been proven to be reasonable (Yuan et al., 2019; Mei et al., 2023), and the methodology has been well validated to the gap-leaping problem (Mei et al., 2019; Mei et al., 2022; Mei et al., 2023). The governing equations are as follows:

$$\boldsymbol{u}_t + \xi \boldsymbol{k} \times \boldsymbol{u} = -\nabla E + A_h \nabla^2 \boldsymbol{u} - R\boldsymbol{u} + \frac{\boldsymbol{\tau}}{\rho_0 h}, \quad (1)$$

$$h_t + \nabla \cdot (h\boldsymbol{u}) = 0, \quad (2)$$

where $u = (\boldsymbol{u}, v)$ is the horizontal velocity vector in the x and y directions, $\xi = f + \boldsymbol{k} \cdot \nabla \times \boldsymbol{u}$ is the absolute vorticity, and $f = f_0 + \beta y$ is the Coriolis parameter on the β-plane with constant Rossby parameter $\beta = 2 \times 10^{-11}$ m^{-1} s^{-1}, where the southern boundary of the model is set as the equator with $f_0 = 0$; $\mathbf{k}$ is the unit vector in the vertical direction, and h is the upper-layer thickness with the initial resting thickness of 300 m, which is close to the thermocline depth of approximately 300–500 m in the western Pacific Ocean; $E = g'h + (u^2 + v^2)/2$ is the total energy, $\boldsymbol{\tau} = (\tau_x, \tau_y)$ is the surface wind stress vector in the x and y directions, $A_h = 300\ m^2\ s^{-1}$ is the horizontal eddy viscosity coefficient, $R = 5 \times 10^{-8}\ s^{-1}$ is the Rayleigh friction coefficient, $\rho_0 = 1024\ kg\ m^{-3}$ is the reference density, and

$g' = 0.031$ m s^{-2} is the reduced gravity. Moreover, the model set is similar to that in Qiu and Chen (2012), and the choices of the lateral viscosity and the Rayleigh friction coefficient are similar to those in Jiang et al. (1995).

The vorticity equation is derived from the cross-differentiation forms of the momentum equations in Equation 1 for vorticity balance analysis first, as follows:

$$\zeta_t + J(\psi, \zeta) + \beta\psi_x = A_h \nabla^2 \zeta - R\zeta + \nabla \times (\frac{\tau}{\rho_0 h}), \quad (3)$$

where $\zeta = \nabla^2\psi$ is the relative vorticity, ψ is the stream function, and J is the Jacobian operator. The effect of the lower-layer circulation is neglected in the hysteresis characteristics of the WBC in the gap-leaping system, and an additional term $-[fh_E/2h]\zeta$ is added to the vorticity equation to estimate the insignificance of the lower-layer circulation, where $h_E = \sqrt{2\nu/f}$ is the Ekman layer depth and $\nu = 0.01$ m^2 s^{-1} is the molecular viscosity (estimating the vertical Ekman layer depth) (Zavala Sanson and Van Heijst, 2002; Cushman-Roisin and Beckers, 2011; Kuehl and Sheremet, 2014; McMahon et al., 2020; McMahon et al., 2021; Mei et al., 2022; Mei et al., 2023). In fact, the horizontal spatial scale is four orders of magnitude larger than the vertical spatial scale in this study. Therefore, the molecular viscosity of about four orders of magnitude lower than the horizontal eddy viscosity coefficient (A_h) is reasonable (Cushman-Roisin and Beckers, 2011).

An idealized rectangular domain separated by a thin meridional barrier into two rectangular basins is adopted, and a thin gap is inserted into the middle of the meridional barrier. The western basin covers 100°–120°E, and the eastern basin, 120°–150°E; both extend from 0° to 30°N. The thin meridional barrier is placed along 120°E with a gap of 2a (~290 km) in width from 13.8°N to 16.4°N. Two meridional islands are inserted into the gap. The Munk layer width $L_M = (A_h/\beta)^{1/3}$ is 24.7 km. Then, the ratio of the half width of the gap to the Munk layer width ($\gamma = a/L_M$) is 5.87, which guarantees the existence of WBC hysteresis (Sheremet, 2001). The inertial boundary layer thickness ($L_I = \sqrt{U_0/\beta}$) is used to estimate the balance between the relative vorticity advection and β effect, where $U_0 (= Q/L)$ is the Sverdrup interior velocity scale, Q is the transport per unit depth of the WBC, and L is the basin length scale (McMahon et al., 2021; Mei et al., 2022; Mei et al., 2023).

The WBC is driven by an idealized zonal wind in the eastern basin, and the transport of the WBC depends on the wind stress strength parameter α_τ, which is controlled by the following equation:

$$\tau_x = -\alpha_\tau \tau_0 \cos(\frac{\pi\phi}{D_{N-S}}), \quad (4)$$

where $\tau_0 = 0.1\ N\ m^{-2}$, ϕ is the latitude, and $D_{N\text{-}S}$ is the latitude interval between the northern and southern boundaries. In the numerical experiments, the integration time of the controlling equation should be long enough for each α_τ for the WBC to reach a steady solution. Then, the transport per unit depth of the WBC (Q) is calculated from the steady solution on the zonal section from 120°E to 121°E at 13.8°N, and the Reynolds number is defined and calculated as $\mathrm{Re} = Q/A_h$. The partial differential equations in Equations 1 and 2 are solved using the finite difference method. The spatial resolution of the model is 0.1°, and the grid convergence has been validated in the numerical experiments (not shown).

In the numerical experiments, the mesoscale eddy of a Gaussian stream function distribution is added to the critical-state WBC as a perturbation. The zonal (u_{eddy}) and meridional (v_{eddy}) velocity components of the eddy are given as follows (Yuan and Li, 2008; Yuan and Wang, 2011; Mei et al., 2022):

$$u_{\mathrm{eddy}} = \psi_0 \frac{y}{r^2} \exp(-\frac{x^2+y^2}{2r^2}), \quad (5)$$

$$v_{\mathrm{eddy}} = -\psi_0 \frac{x}{r^2} \exp(-\frac{x^2+y^2}{2r^2}), \quad (6)$$

where ψ_0 is the maximum stream function value of the mesoscale eddy at the center, with positive (negative) ψ_0 representing an anticyclonic (a cyclonic) eddy, and r is the distance of the maximum azimuthal velocity of the eddy at 80 km from the eddy center.

3 Results

3.1 Hysteresis of WBC with two islands in the gap

In order to study the hysteresis of the WBC with two islands in the gap, numerous numerical experiments are designed, and the results are compared with those of Mei et al. (2019); Mei et al. (2022). We place two islands of ~22 km in meridional width on the gap, where the position of the northern island is from 15° to 15.2°N, and that of the southern island is from 14° to 14.2°N, resembling the central Batanes Island and the southern Babuyan Island in the Luzon Strait. Figure 2 shows the hysteresis curves of the WBC in the no-island, one-island, and two-island cases, where X_P represents the farthest distance to the west of the $\psi = Q/2$ streamline of the WBC main stream into the western basin from the gap. In the numerical experiments, α_τ is first increased with an interval of 0.01 from 0.18 to 0.83 [the wind stress increasing stage, as in Mei et al. (2019)], and then, it gradually decreased from a supercritical value of more than 0.83 to 0.18 [the wind stress decreasing stage, as in Mei et al. (2019)]. Note that the steady-state solution of the earlier integration is used as the initial condition of the later integration to retain the historical WBC status, as in Mei et al. (2019); Mei et al. (2022). For each α_τ, the Re is calculated for both the cases in the wind stress increasing and decreasing stages.

During the wind stress increasing stage, Figure 2 shows that the WBC flow state experiences three types of regimes as Re is increased, including the penetrating, periodic eddy-shedding, and leaping regimes. First, the WBC intrudes into the western basin as an anticyclonic loop current near the gap at low Re. Then, the WBC path experiences a first transition from the penetrating to the periodic eddy-shedding regime at $\mathrm{Re}_{C\text{-}2} = 31$ (the lower Hopf bifurcation) for the two-island case, corresponding to the multivalued hysteresis curves, which indicates the distances of the farthest and closest WBC intrusion into the western basin between the two adjacent half periods during one eddy-shedding process. At

10.3389/fmars.2023.1147292

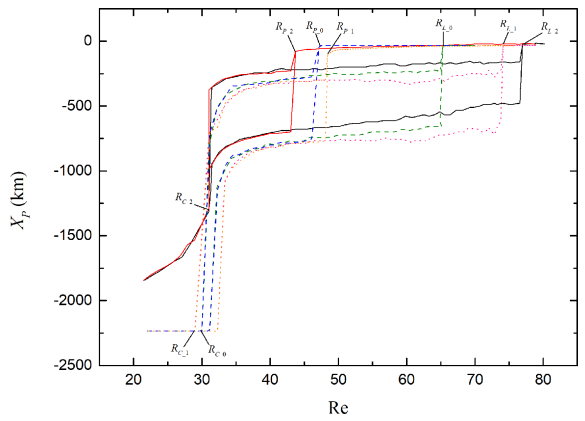

FIGURE 2
Hysteresis curves of the WBC with no island, one island, and two islands in the gap, where X_P is the westernmost position of the $\psi = Q/2$ streamline of the WBC, with 0 standing for the position of the barrier; the Reynolds number is defined as $Re = Q/A_h$; $Re_{C\text{-}2}$ ($Re_{C\text{-}0}$, $Re_{C\text{-}1}$) is the critical value of the WBC in the gap with two islands (no island, one island) shifting from the penetrating to the eddy-shedding regime. $Re_{L\text{-}2}$ ($Re_{L\text{-}0}$, $Re_{L\text{-}1}$) is the critical value of the WBC in the gap with two islands (no island, one island) shifting from the eddy-shedding to leaping regime. $Re_{P\text{-}2}$ ($Re_{P\text{-}0}$, $Re_{P\text{-}1}$) is the critical value of the WBC in the gap with two islands (no island, one island) shifting from the leaping to eddy-shedding regime. The double curves indicate the WBC in the periodic eddy-shedding regime. WBC, western boundary current.

that moment, the WBC begins to intrude into the western basin as a periodic eddy-shedding path. It can be seen in Figure 2 that the lower Hopf bifurcation is almost unchanged for the three cases regardless of the island's presence in the gap, where the corresponding Re of the no-island and one-island cases are $Re_{C\text{-}0} = 30$ and $Re_{C\text{-}1} = 29$, respectively. When the Re is increased to be more than another critical value Re_L, the WBC experiences a second transition from the periodic eddy-shedding to leaping regimes at $Re_{L\text{-}2} = 77$ (the upper Hopf bifurcation). Then, the WBC leaps across the gap, and the hysteresis curve changes to be a single-value curve again. As a result, the hysteresis curves suggest that the presence of the two islands in the gap facilitates the WBC intrusion into the western basin in the eddy-shedding regime compared with the no-island case ($Re_{L\text{-}0} = 65$) and one-island case ($Re_{L\text{-}1} = 74$) in the wind stress increasing stage, because the difference of Re (defined as $\Delta Re_{IN} = Re_L\text{-}Re_C$ in the wind stress increasing stage) between the upper and lower Hopf bifurcations is $\Delta Re_{2,IN} > \Delta Re_{1,IN} > \Delta Re_{0,IN}$.

During the wind stress decreasing stage, the hysteresis curves indicate that the WBC also experiences the above-mentioned three flow regimes as Re is decreased. When Re is reduced from a supercritical value to $Re_{P\text{-}0} = 46$, $Re_{P\text{-}1} = 48$, and $Re_{P\text{-}2} = 43$, respectively, the WBC shifts regimes from the leaping path to the periodic eddy-shedding path for the no-island case, one-island case, and two-island case. The results suggest that the WBC hysteresis occurs in a specific interval of Re in this situation, i.e., the eddy-shedding regime and leaping regime of the WBC coexist at the same Re in the range of (Re_P, Re_L). As Re is further reduced to Re_C, the transition of the WBC path from the periodic eddy-shedding to penetrating (an anticyclonic loop current) regime occurs. In this case, however, the presence of two islands in the gap is unfavorable to the WBC to intrude into the western basin by shedding eddies compared with the no-island and one-island cases, because the difference of Re (defined as $\Delta Re_{DE} = Re_P - Re_C$ in the wind stress decreasing stage) is $\Delta Re_{1,DE} > \Delta Re_{0,DE} > \Delta Re_{2,DE}$.

From the above results, on the one hand, it can be concluded that the presence of two islands in the gap facilitates the WBC intrusion compared with the no-island case, but it is unfavorable to the WBC intrusion compared with the one-island case, by shedding eddies into the western basin. This is evidenced by the comparison of the parameter space of the WBC in the eddy-shedding regime, i.e., $(\Delta Re_{1,IN} + \Delta Re_{1,DE}) > (\Delta Re_{2,IN} + \Delta Re_{2,DE}) > (\Delta Re_{0,IN} + \Delta Re_{0,DE})$. On the other hand, the farthest intrusive distance (corresponding to the maximum value X_P) of approximately 1,700 km for the two-island case is smaller than that of approximately 2,200 km for both the no-island and one-island cases in Figure 2. This indicates that the presence of the southern island hinders the intrusive distance of the WBC into the western basin to some extent, and the result is in accord with the realistic model result in Metzger and Hurlburt (2001).

The time evolution of the WBC pattern in the vicinity of the gap with two islands under different Re is shown in Figure 3. In the wind stress increasing stage, the WBC begins to intrude into the western basin as a loop current at Re = 24 (Figure 3A). Then, the WBC starts to the shed eddies at Re = 31, and it retains the eddy-shedding path until at Re = 75, as shown in Figure 3B. Note that the WBC mainly flows into the western basin through the gap between the northern and southern islands, with a little of WBC water leaking into the western basin through the narrow gap between the southern island and the southern barrier. As Re is increased to $Re_{L\text{-}2} = 77$ (Figure 3C), the WBC transforms to leap across the gap. In the wind stress decreasing stage, the WBC stays in the leaping regime until Re is reduced to $Re_{P\text{-}2} = 43$, where the WBC path is transited to the eddy-shedding pattern (Figure 3E). It can be seen that the eddy-shedding and leaping patterns of the WBC coexist at the same Re (=75) in Figures 3B, D, which indicates that WBC hysteresis occurs at that moment. When Re is further decreased to Re = 24, the WBC intrudes into the western basin as a loop current again (Figure 3F). According to the above experiments, the inertial boundary layer thickness L_I changes from approximately 9.5 to 19.6 km, which is smaller than the Munk boundary layer thickness (24.7 km). This indicates that horizontal friction dominated the advection and Rayleigh friction (McMahon et al., 2021; Mei et al., 2022; Mei et al., 2023).

3.2 Impact of mesoscale eddy on the WBC regime shifts with two islands in the gap

In this section, the impact of two islands in the gap on the critical-state WBC transition during the WBC–eddy interaction is studied and compared with that of the no-island case (Yuan and Wang, 2011) and the one-island case (Mei et al., 2022). The impact of north–south locations of the mesoscale eddy on the critical-state WBC path is also studied. As shown in Figure 2, the WBC begins to shift regimes from the eddy-shedding path to the leaping path at

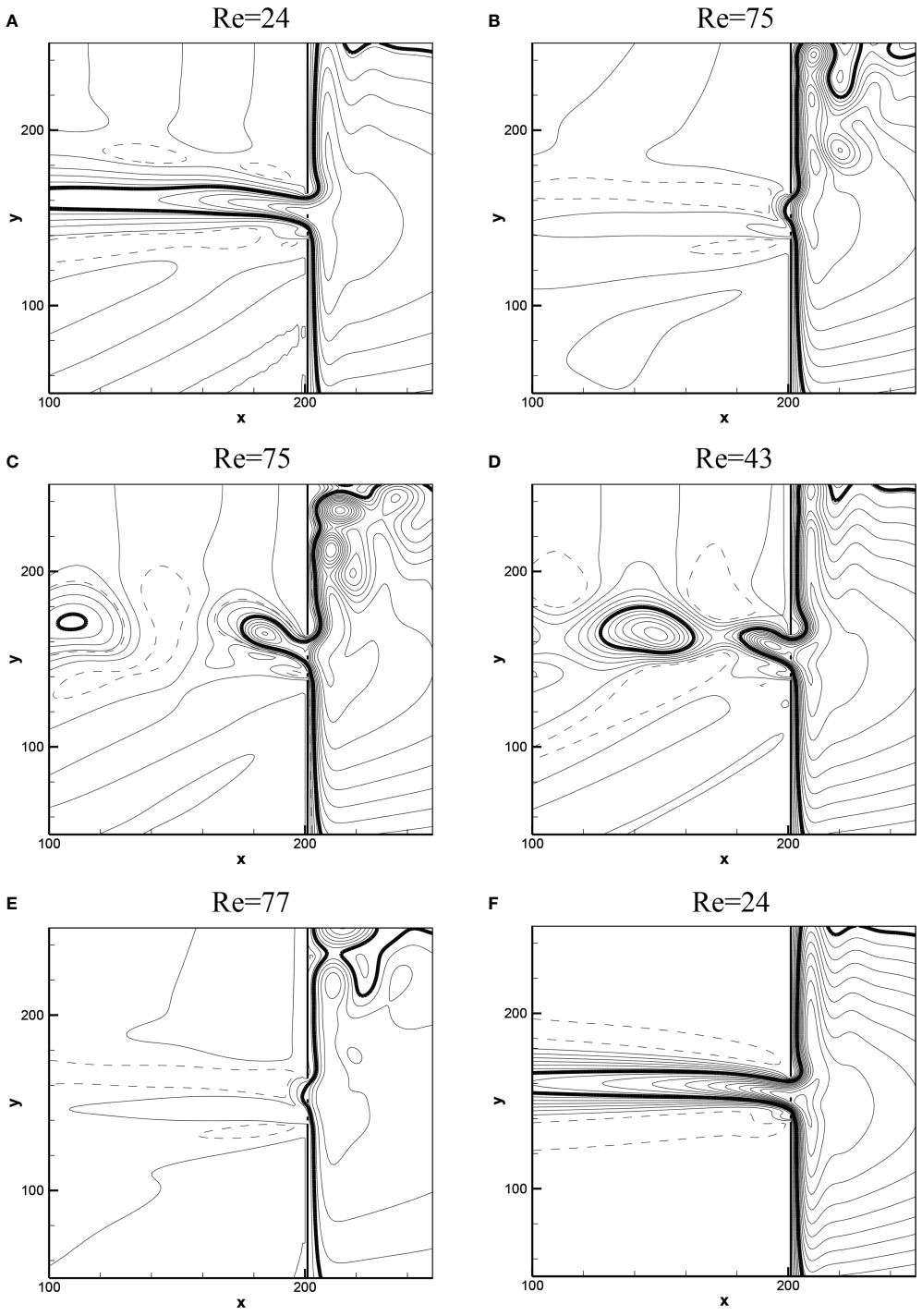

FIGURE 3
Time evolution of the WBC in the vicinity of the gap with two islands under different Re. **(A–C)** The WBC pattern in the wind stress increasing stage and **(D, F)** that in the wind stress decreasing stage. **(C, E)** The $Re_{L\text{-}2}$ and $Re_{P\text{-}2}$ positions in Figure 1. The bold curve represents the $\psi = Q/2$ streamline of the WBC and shed eddy. WBC, western boundary current.

$Re_{L\text{-}2}$ = 77 and from the leaping path to the eddy-shedding path at $Re_{P\text{-}2}$ = 43. Then, the steady solution of the critical-state WBC at Re = 76 (Re = 44) in the wind stress increasing (decreasing) stage is used as the background flow. A mesoscale eddy is inserted 300 km east of the gap into the critical-state WBC solution as the initial condition (Yuan and Li, 2008; Yuan and Wang, 2011; Mei et al., 2022).

3.2.1 From penetration to leap

First, when the WBC is critical from the eddy-shedding to leaping regime, an anticyclonic eddy is released due east of the gap center, and then it moves westward on the β plane. The time evolution of the WBC flow pattern in the vicinity of the gap is shown in Figure 4. In this case, the critical strength of the eddy that can induce the WBC transition from penetration to leap is ψ_c =

26,000 m^2 s^{-1}. As the anticyclonic eddy moves to the gap and interacts with the WBC, the critical WBC gradually stops at the shed eddies and begins to leap across the gap at approximately 700 days. Then, the WBC remains in the leaping regime permanently. The left fling of the anticyclonic eddy enhances the WBC speed as well as the meridional advection at the entrance of the gap, and then it induces the WBC transition, similar as in Yuan and Wang (2011) and Mei et al. (2022).

The dynamics of the WBC transition is analyzed by extracting each vorticity term from Equation 3 at a grid point nearest to X_P, as shown in Figure 5. At the initial stage of the numerical experiment, all the vorticity balance terms are oscillatory. As the anticyclonic eddy interacts fully with the WBC at approximately day 700, the vorticity balance shows that the meridional advection term increases by one order of magnitude, and the vorticity balance is mainly between the beta term and the other terms. Then, the WBC transition from the eddy-shedding regime to leaping regime occurs. In the above experiment, the lower-layer circulation estimated by the additional term $-[fh_E/2h]\zeta$ is at least one order of magnitude smaller than the meridional advection and β terms (not shown). Further, the observations and model results show that the barotropic component of full-depth current and the lower-layer circulation in the SCS are both one order of magnitude smaller than the velocity of the upper-layer circulation, as mentioned in Mei et al. (2023). This illustrates the lower-layer circulation is negligible.

We also examine the impact of a central cyclonic eddy on the regime shifts of the WBC critical from the eddy-shedding to leaping regime. The critical strength of the cyclonic eddy inducing the WBC transition is ψ_c = 28,000 m^2 s^{-1}. Figure 6 shows the time evolution of the critical WBC impinged by the cyclonic eddy near the gap. When the westward-moving cyclonic eddy approaches the gap and impinges on the WBC, the eddy shape is squeezed and distorted,

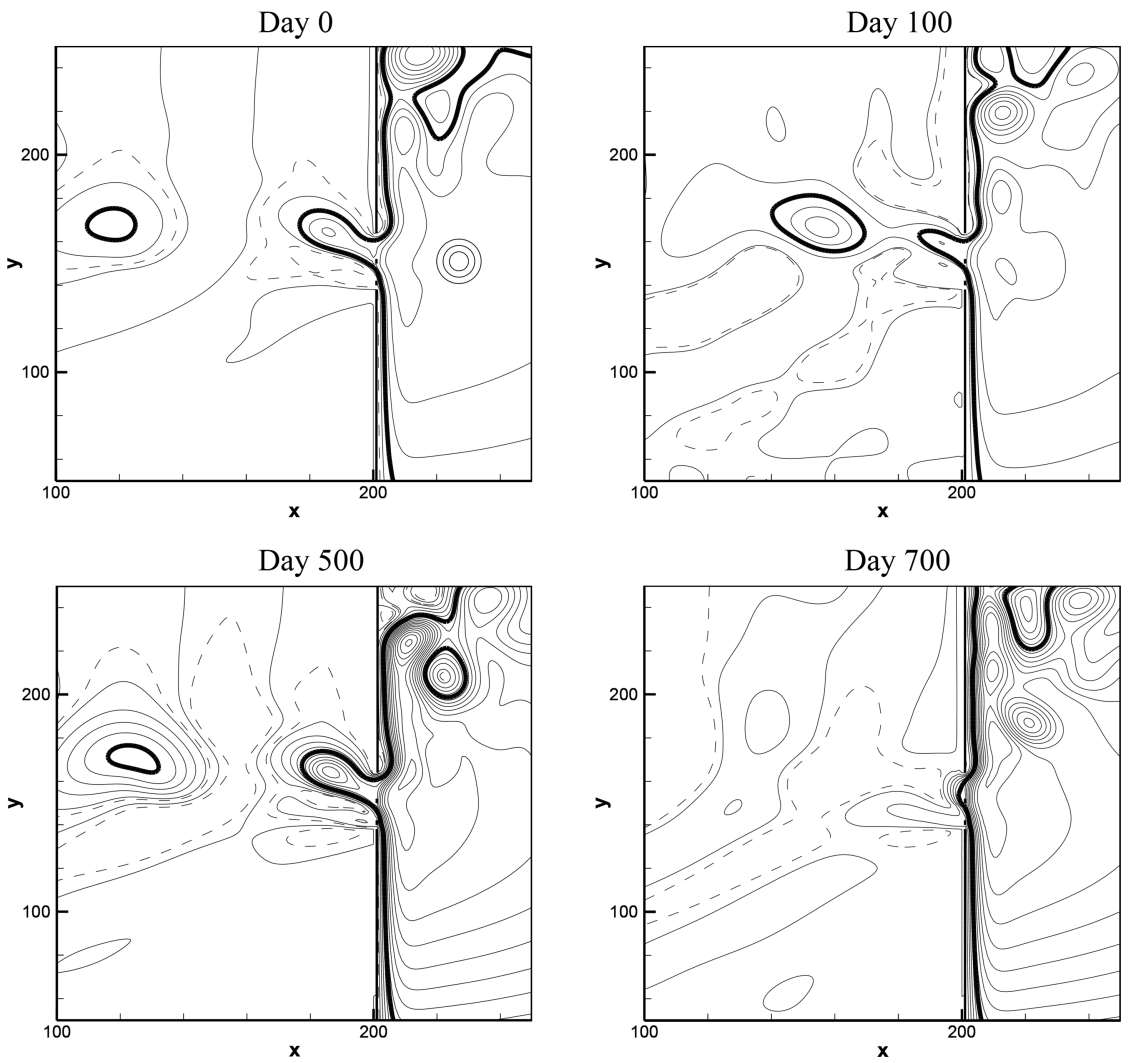

FIGURE 4
Time evolution of the WBC critical from the eddy-shedding to leaping regime at Re = 76 impinged by an anticyclonic eddy in the vicinity of the gap with two islands. An initial anticyclonic eddy with a radius of approximately 80 km is inserted 300 km east of the gap into the background flow, and it propagates toward the gap. The critical strength of the eddy (ψ_c = 26,000 m^2 s^{-1}) is the minimum value that can induce the critical WBC transition from penetration to leap. WBC, western boundary current.

and then the eddy energy is almost absorbed by the WBC to transport westward and northward. As the right fling of the eddy approaches the gap area, the WBC speed at the entrance of the gap is enhanced by the northward current of the eddy, and then the WBC turns to leap across the gap at approximately day 900.

Figure 7 shows the vorticity balance analysis of the cyclonic eddy–WBC interaction near X_P. All the vorticity balance terms start to oscillate until at approximately day 900 when the beta and meridional advection terms increase by one order of magnitude. Then, the vorticity balance is mainly the increased beta term balances the increased meridional advection and viscosity terms. As the WBC transition occurs, the WBC maintains the leaping path over time. Note that the cyclonic eddy takes more time to induce the WBC regime shift than that in Figure 5. This is because the right fling of the cyclonic eddy takes more time to reach the gap than that of the left fling of the anticyclonic eddy.

Next, the impact of variable north–south locations of the mesoscale eddy on the critical-state WBC transition is studied with the presence of two islands in the gap-leaping system. In the following numerical experiments, the eddies are specified unchangeably 300 km east of the gap in the zonal direction, but their north–south locations are changed continuously in the meridional direction. The critical strength of the eddy (ψ_c) that is able to induce the WBC transition is normalized by the critical WBC strength, i.e., $\gamma = \psi_c/Q_c$. The dimensionless parameter $\lambda(=L_i/L_g)$ is defined to indicate the location of the initial eddy, where L_i is the meridional distance between the latitude of the eddy center and that of the northern tip of the southern barrier, and L_g is the gap width. The critical strength of the eddy inducing the critical WBC transition from the periodic eddy-shedding to leaping regime as a function of λ for the two-island case is shown in Figure 8. First, the WBC regime shift is most sensitive to the anticyclonic eddy due east of the gap center, and it is least sensitive to the anticyclonic eddy approaching the gap downstream of the WBC (Figure 8A). The least sensitive location of the anticyclonic eddy is in accord with the no-island case in Yuan and Wang (2011) and one-island case in Mei et al. (2022), where the northern anticyclonic eddy can induce the critical-state WBC transition more difficultly than from the center and south of the gap. Second, the regime shift of the WBC is most sensitive to the cyclonic eddy from the south of the gap and least sensitive to the cyclonic eddy downstream of the WBC (Figure 8B). The most sensitive location of the cyclonic eddy is in accord with the no-island case in Yuan and Wang (2011) but is opposite to the one-island case in Mei et al. (2022).

3.2.2 From leap to penetration

In this subsection, we examine the influence of a mesoscale eddy on the regime shifts of the WBC critical from the leaping to eddy-shedding path. When a cyclonic eddy is inserted 300 km due east of the gap center as the initial condition, the critical eddy strength that can induce the WBC transition from leap to penetration is ψ_c = 28,000 $m^2\ s^{-1}$. Figure 9 shows the time evolution of the critical WBC pattern at Re = 44 impinged by the cyclonic eddy in the vicinity of the gap with two islands. At approximately day 700, the cyclonic eddy is eventually absorbed by the WBC, and the southward current of the left fling of the eddy reduces the northward speed of the WBC at the entrance of the gap, which induces the WBC regime shifts. Then, the WBC pattern is permanently shifted from the leaping regime to the penetrating regime.

The vorticity balance of the cyclonic eddy–WBC interaction is analyzed in Figure 10. As the cyclonic eddy moves westward and eventually approaches the gap area, it reduces the meridional advection term of the WBC during the interactional process, and then the decreased beta term is mainly balanced by the decreased meridional advection and viscosity terms when the WBC pattern translates to the eddy-shedding path. At last, all the vorticity balance terms appear to be periodic.

Then, the impact of an anticyclonic eddy on the critical WBC path is studied as well. In this case, the critical strength of the anticyclonic eddy is ψ_c = 41,000 $m^2\ s^{-1}$. Figure 11 shows the time evolution of the critical WBC pattern impinged by the anticyclonic eddy in the vicinity of the gap between the two islands. It can be seen that the WBC shifts regimes under the perturbation of the eddy. It is the right fling of the anticyclonic eddy that reduces the

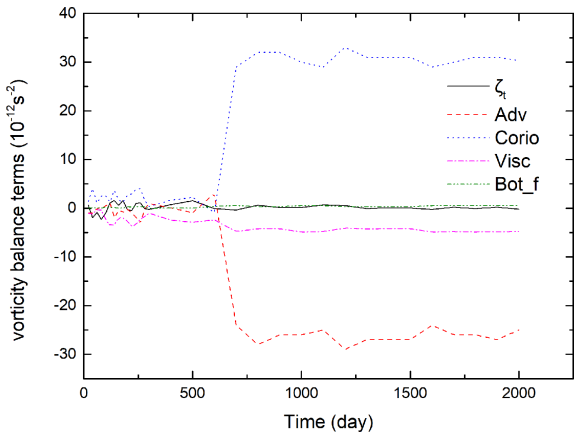

FIGURE 5
Time evolution of the vorticity balance terms near X_P during the interaction of the anticyclonic eddy and the WBC critical from penetration to leap at Re = 76 in the vicinity of the gap with two islands. WBC, western boundary current.

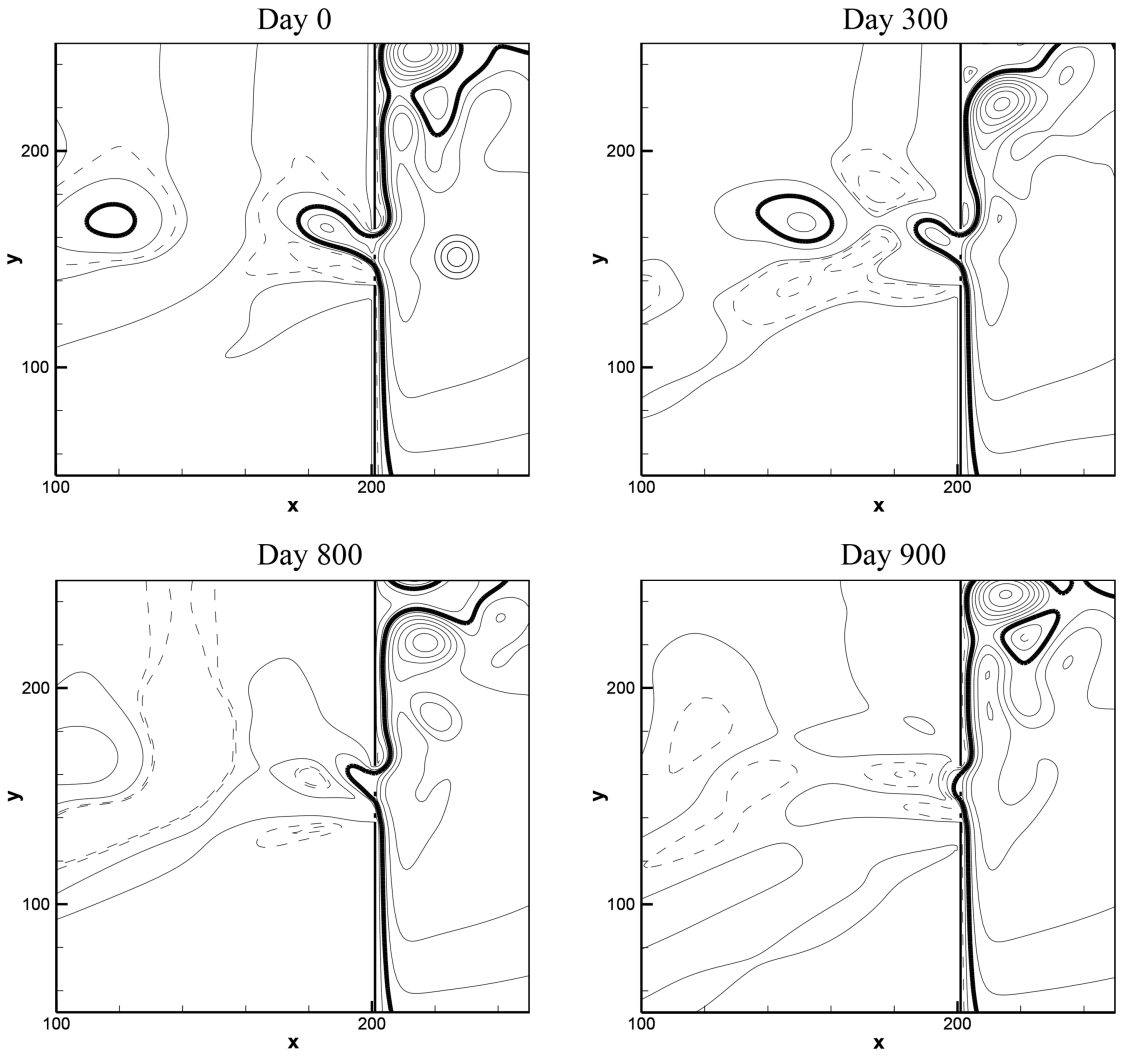

FIGURE 6
Same as Figure 4, except for the critical WBC pattern impinged by a cyclonic eddy. The critical strength of the eddy is ψ_c = 28,000 m^2 s^{-1}. WBC, western boundary current.

northward current of the WBC as well as the meridional advection at the entrance of the gap, so as to promote the WBC intrusion into the western basin and induce the WBC transition. The result is similar to that in Mei et al. (2022), where the anticyclonic eddies from the east were able to induce the critical WBC regime shifts from the leaping to eddy-shedding regime when one island is present in the gap. However, it is opposite to Yuan and Wang (2011), who concluded that the anticyclonic eddies could not induce the WBC transition from the leap to penetration.

Figure 12 shows the vorticity balance analysis of the anticyclonic eddy–WBC interaction and indicates that the decreased beta term is balanced by both the decreased meridional advection and viscosity terms when the WBC path shifts from the leaping regime to the eddy-shedding regime. Then, the WBC keeps the penetrating path, and all vorticity terms appear to be periodic as time elapses.

At last, we examine the critical-state WBC regime shifts from leap to penetration perturbed by the mesoscale eddy of variable north–south locations. The critical strength of the eddy inducing the WBC transition as a function of λ for the two-island case is shown in Figure 13. It can be seen that the critical strength of the cyclonic eddy from the south of the gap is almost unchanged (Figure 13A). The WBC transition is most sensitive to the southern cyclonic eddies and least sensitive to the northern cyclonic eddies, which is in accord with the one-island case in Mei et al. (2022). Moreover, the most sensitive location of the cyclonic eddy is in accord with the no-island case in Yuan and Wang (2011). However, the northern cyclonic eddy cannot induce the WBC transition from leap to penetration in their study. However, the critical strength of the anticyclonic eddy increases as λ increases (Figure 13B). The regime shift of the WBC is most sensitive to the anticyclonic eddy upstream of the WBC and least

10.3389/fmars.2023.1147292

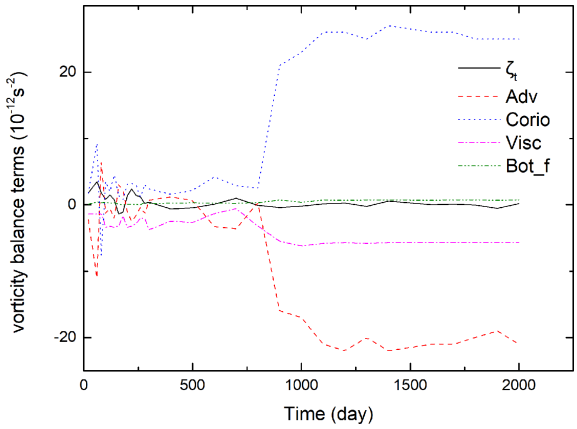

FIGURE 7
Same as Figure 5, except for the cyclonic eddy–WBC interaction. WBC, western boundary current.

sensitive to that from the northern gap, which is opposite to the one-island case in Mei et al. (2022).

4 Conclusions and discussion

In this paper, the hysteresis of the WBC flowing across the gap with two islands and the dynamics of the mesoscale eddy–WBC interaction affected by the two islands are studied using the nonlinear 1.5-layer ocean model. The hysteresis curves show that the lower Hopf bifurcation of the WBC transition exhibits no differences in the two-island case compared with the existing results in the no-island and one-island cases. The critical Re of the upper Hopf bifurcation for the two-island case is larger than that of the no-island and one-island cases. However, the critical Re of the WBC transiting from the leaping to eddy-shedding regime is

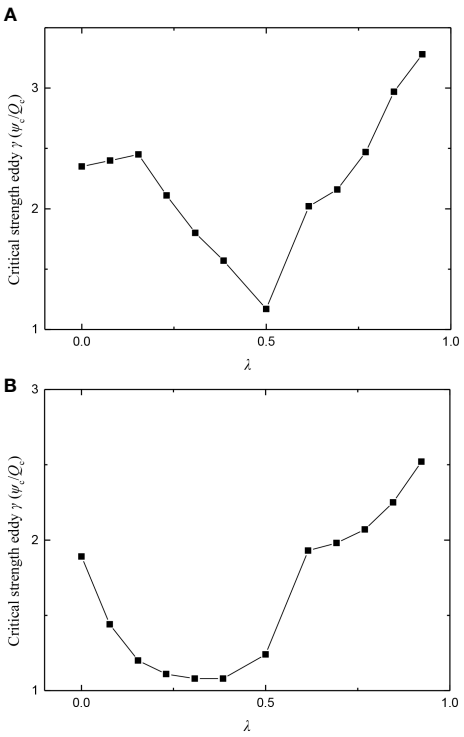

FIGURE 8
The dimensionless critical strength (γ) of the anticyclonic eddy **(A)** and the cyclonic eddy **(B)** inducing the critical WBC transition from the penetrating to leaping regime as a function of λ ($=L_i/L_g$), where $\gamma = \psi_c/Q_c$ represents the critical strength of the eddy (ψ_c) normalized by the critical WBC strength (Q_c), L_i is the meridional distance between the latitude of the eddy center and the latitude of the northern tip of the southern barrier, and L_g is the gap width. WBC, western boundary current.

10.3389/fmars.2023.1147292

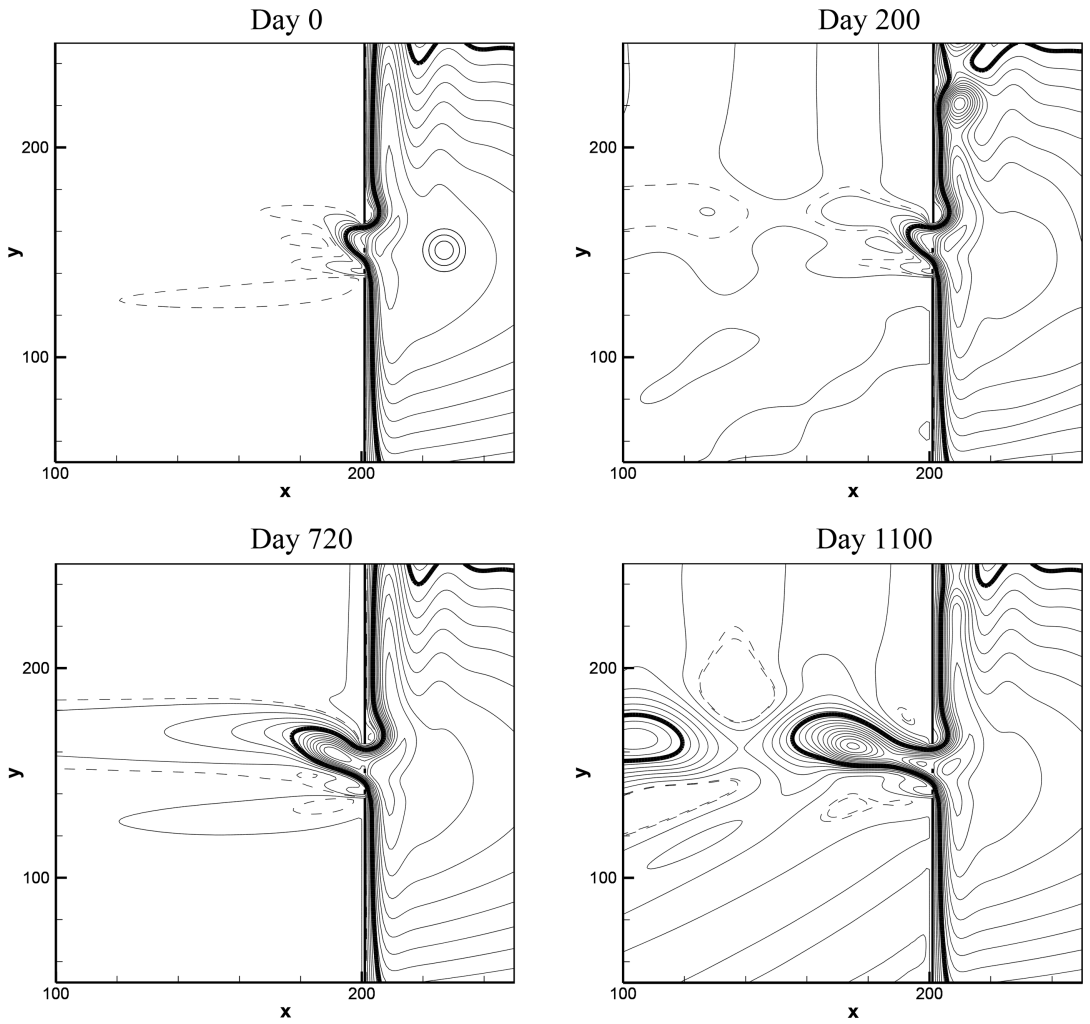

FIGURE 9
Time evolution of the WBC critical from the leaping to eddy-shedding regime at Re = 44 impinged by a cyclonic eddy in the vicinity of the gap with two islands. The cyclonic eddy with a radius of 80 km is inserted 300 km east of the gap into background flow and propagates toward the gap. The critical strength of the eddy is ψ_c = 28,000 m^2 s^{-1} to induce the critical WBC transition from leap to penetration. WBC, western boundary current.

smaller than that of the no-island and one-island cases. Considering the parameter space of the WBC in the eddy-shedding regime, it is found that the presence of two islands in the gap is favorable to the WBC intrusion by shedding eddies compared with the no-island case, but it is unfavorable to the WBC intrusion compared with the one-island case because the size of order of the parameter is $(\Delta Re_{1,IN} + \Delta Re_{1,DE}) > (\Delta Re_{2,IN} + \Delta Re_{2,DE}) > (\Delta Re_{0,IN} + \Delta Re_{0,DE})$.

The westward-moving mesoscale eddies from the east of the gap are able to induce the critical WBC transition with the two islands' presence in the gap. Both the anticyclonic and cyclonic eddies can induce the critical WBC shifting from the eddy-shedding regime to leaping regime and vice versa. The dynamics revealed by the vorticity balance show all the vorticity terms oscillate periodically for the WBC in the eddy-shedding regime, and then the meridional advection and viscosity terms are increased to balance the increased beta term perturbed by the eddy, which induces the WBC transition from penetration to leap. Conversely, the decreased meridional advection and viscosity terms are balanced by the decreased beta term perturbed by the eddy, which is responsible for the WBC transition from leap to penetration.

The model results suggest that the mesoscale eddy with variable north–south locations has a significant impact on the critical-state WBC transition with the presence of two islands in the gap-leaping system. When the critical WBC is shifted from the eddy-shedding to leaping regime, the WBC transition is most sensitive to the

10.3389/fmars.2023.1147292

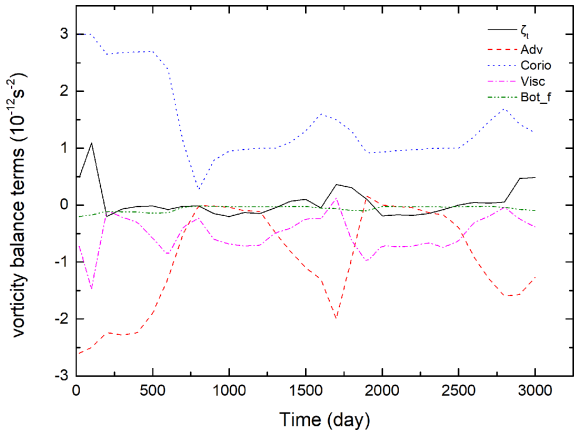

FIGURE 10
Time evolution of the vorticity balance terms near X_P during the interaction between a cyclonic eddy with the WBC critical from leap to penetration at Re = 44 in the vicinity of the gap with two islands. WBC, western boundary current.

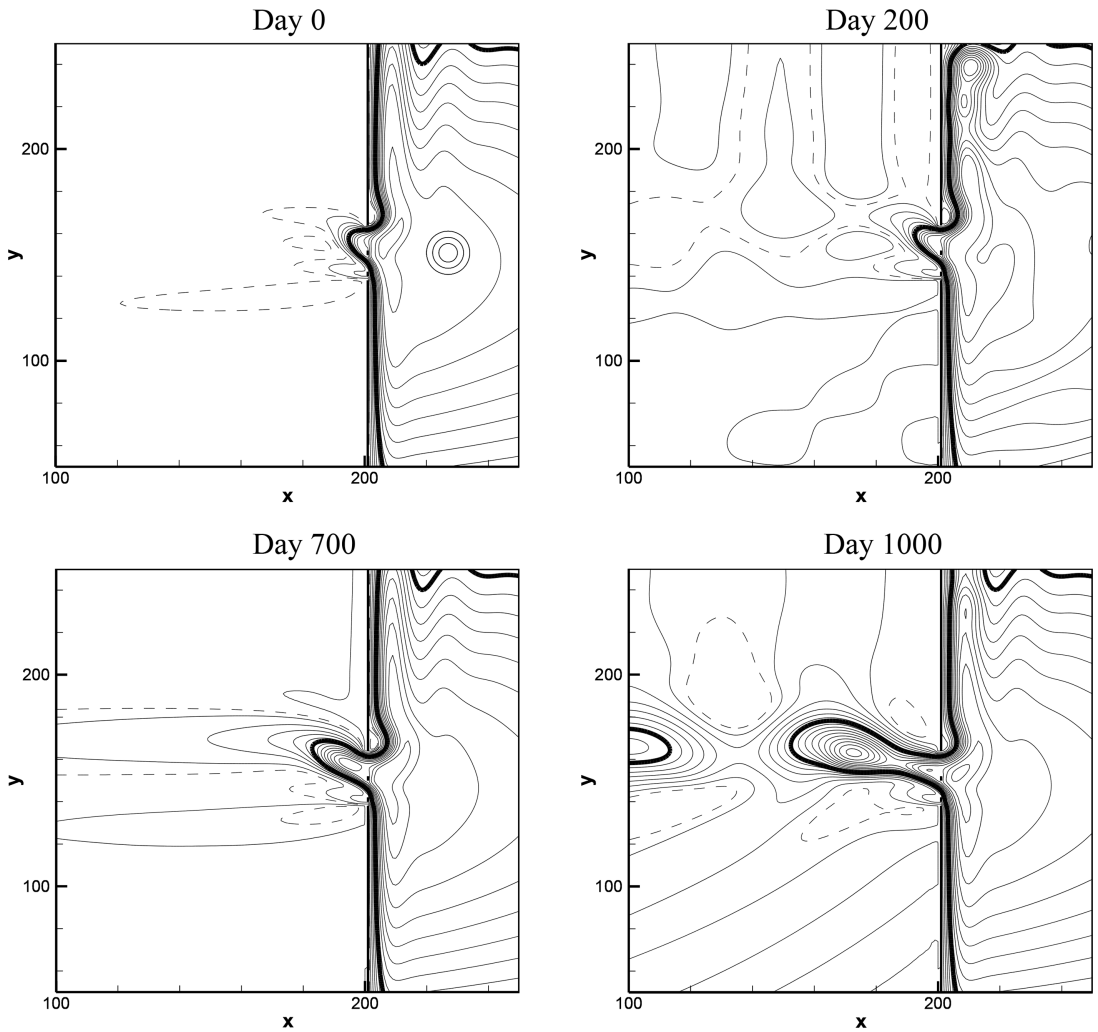

FIGURE 11
Same as Figure 9, except for the critical WBC path impinged by an anticyclonic eddy. The critical strength of the eddy is ψ_c = 41,000 m^2 s^{-1}. WBC, western boundary current.

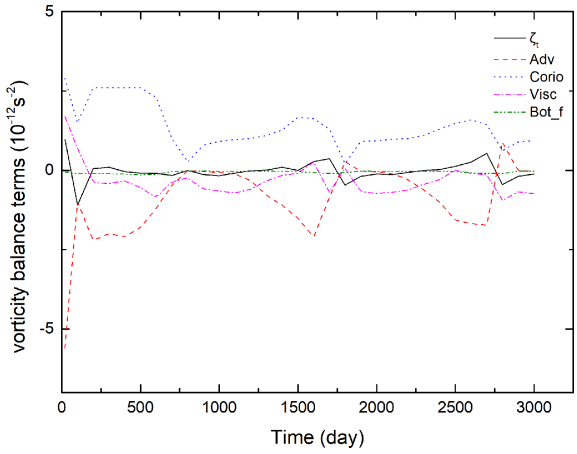

FIGURE 12
Same as Figure 10, except for the anticyclonic eddy–WBC interaction. WBC, western boundary current.

anticyclonic eddy due east of the gap center and is most sensitive to the cyclonic eddy from the south of the gap. It is least sensitive to the anticyclonic and cyclonic eddies downstream of the WBC. When the critical WBC is shifted from the leaping to eddy-shedding regime, the cyclonic eddies from the southern part of the gap exhibit no obvious difference in the critical eddy strength in inducing the critical WBC transition. In this case, the critical WBC regime shifts are most sensitive to the southern cyclonic eddies and least sensitive to the northern cyclonic eddies. The regime shift of the WBC is most sensitive to the anticyclonic eddy upstream of the WBC and least sensitive to that from the northern gap.

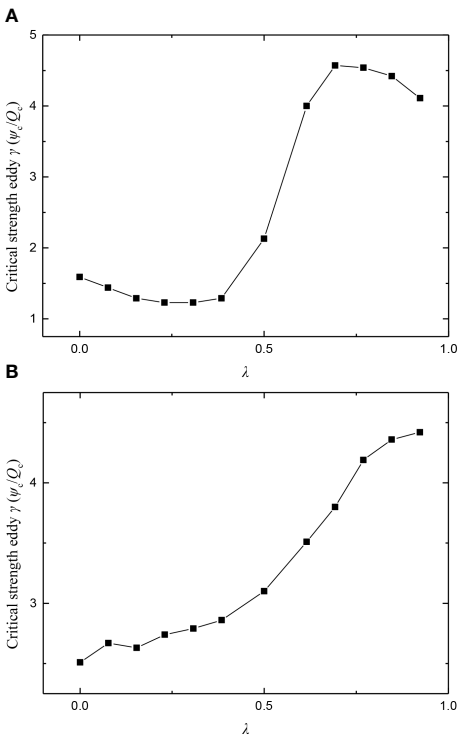

FIGURE 13
The dimensionless critical strength (γ) of the cyclonic eddy **(A)** and the anticyclonic eddy **(B)** inducing the critical WBC transition from the leaping to penetrating regime as a function of λ. WBC, western boundary current.

This study improves our understanding of the dynamics in the regional ocean that the Kuroshio passes by the Luzon Strait in the leaping or penetrating regime. Mei et al. (2022) suggested that the chance of the WBC in the leaping regime is equal to that in the eddy-shedding regime as one island presents in the gap, which overestimates the observation that the time of the Kuroshio in the leaping regime was about twice of that in the penetrating regime in the real world, as summarized in Yuan et al. (2006). Meanwhile, Mei et al. (2022) suspected that the southern Babuyan Island may prevent the Kuroshio from intruding into the SCS to some extent, which was confirmed by the model results in Mei et al. (2019), where only a southern island presents in the gap. The present results with two islands in the gap support that the southern island facilitates the WBC to leap across the gap compared with the one-island case in Mei et al. (2022), despite the chance of the WBC in the leaping or penetrating regime perturbed by the mesoscale eddy is not changed. This may force the WBC to remain in the leaping regime for a longer time than that in the one-island case and should be confirmed in reality in the future. Moreover, the impact of the meridional location of the mesoscale eddy approaching the gap with two islands exhibits an obvious difference in comparison with the no-island case (Yuan and Wang, 2011) and the one-island case (Mei et al., 2022). This indicates that the southern island in the gap affects the eddy–WBC interaction to some extent. In fact, the two-island model is closer to the reality in the Luzon Strait in this study. Obviously, further study using realistic models or observations on the interactions of the mesoscale eddy and the Kuroshio needs to be carried out in the future.

Data availability statement

The original contributions presented in the study are included in the article/supplementary material. Further inquiries can be directed to the corresponding authors.

Author contributions

KL performed the numerical simulation and data analysis and wrote the first draft of the manuscript. HM and QL proposed the work ideas and contributed to the numerical simulation, data analysis, and writing. XW and JD contributed to the data analysis. All authors contributed to the article and approved the submitted version.

Funding

This research is supported by the National Natural Science Foundation of China (Nos. 42076005 and 41706003) and the Natural Science Foundation of Jiangsu Province (No. BK20210885).

Conflict of interest

The authors declare that the research was conducted in the absence of any commercial or financial relationships that could be construed as a potential conflict of interest.

Publisher's note

References

Caruso, M. J., Gawarkiewicz, G. G., and Beardsley, R. C. (2006). Interannual variability of the kuroshio intrusion in the south China Sea. *J. Oceanogr.* 62, 559–575. doi: 10.1007/s10872-006-0076-0

Chern, C. S., and Wang, J. (2005). Interactions of mesoscale eddy and western boundary current: A reduced-gravity numerical model study. *J. Oceanogr.* 61 (2), 271–282. doi: 10.1007/s10872-005-0037-z

Cushman-Roisin, B., and Beckers, J. M. (2011). *Introduction to geophysical fluid dynamics: physical and numerical aspects* (New York: Academic press), 223–224.

Huang, Z., Liu, H., Lin, P., and Hu, J. (2017). Influence of island chains on the kuroshio intrusion in the Luzon strait. *Adv. Atmos. Sci.* 34 (3), 397–410. doi: 10.1007/s00376-016-6159-y

Jiang, S., Jin, F., and Ghil, M. (1995). Multiple equilibria, periodic, and aperiodic solutions in a wind-driven, double-gyre, shallow water model. *J. Phys. Oceanogr.* 25 (5), 764–786. doi: 10.1175/1520-0485(1995)025<0764:MEPAAS>2.0.CO;2

Kuehl, J. J., and Sheremet, V. A. (2009). Identification of a cusp catastrophe in a gap-leaping western boundary current. *J. Mar. Res.* 67 (1), 25–42. doi: 10.1357/002224009788597908

Kuehl, J. J., and Sheremet, V. A. (2014). Two-layer gap-leaping oceanic boundary currents: experimental investigation. *J. fluid Mech.* 740, 97–113. doi: 10.1017/jfm.2013.645

Kuehl, J. J., and Sheremet, V. A. (2022). Effect of the coastline geometry on the boundary currents intruding through the gap. *Fluids* 7 (2), 71. doi: 10.3390/fluids7020071

Kuo, Y. C., and Chern, C. S. (2011). Numerical study on the interactions between a mesoscale eddy and a western boundary current. *J. oceanogr.* 67 (3), 263–272. doi: 10.1007/s10872-011-0026-3

Liang, W. D., Yang, Y. J., Tang, T. Y., and Chuang, W. S. (2008). Kuroshio in the Luzon strait. *J. Geophys. Res.: Oceans* 113 (C08048). doi: 10.1029/2007JC004609

McMahon, C. W., Kuehl, J. J., and Sheremet, V. A. (2020). A viscous, two-layer western boundary current structure function. *Fluids* 5 (2), 63. doi: 10.3390/fluids5020063

McMahon, C. W., Kuehl, J. J., and Sheremet, V. A. (2021). Dynamics of gap-leaping Western boundary currents with throughflow forcing. *J. Phys. Oceanogr.* 51 (7), 2243–2256. doi: 10.1175/JPO-D-20-0216.1

Mei, H., Li, K., Liu, Q., Wang, B., and Wu, X. (2023). Interaction of a hysteresis western boundary current with a large-scale marginal sea circulation in a gap-leaping system. *J. Phys. Oceanogr.* 53 (3), 943–957 doi: 10.1175/JPO-D-22-0194.1

Mei, H., Qi, Y., Cheng, X., Wu, X., and Wang, Q. (2022). Nonlinear dynamics of a hysteresis Western boundary current perturbed by a mesoscale eddy at a gap with an island. *J. Phys. Oceanogr.* 52, 1992–2007. doi: 10.1175/JPO-D-22-0016.1

Mei, H., Qi, Y., Qiu, B., Cheng, X., and Wu, X. (2019). Influence of an island on hysteresis of a western boundary current flowing across a gap. *J. Phys. Oceanogr.* 49 (5), 1353–1366. doi: 10.1175/JPO-D-18-0116.1

Metzger, E. J., and Hurlburt, H. E. (2001). The importance of high horizontal resolution and accurate coastline geometry in modeling south China Sea inflow. *Geophys. Res. Lett.* 28 (6), 1059–1062. doi: 10.1029/2000GL012396

Nan, F., He, Z., Zhou, H., and Wang, D. (2011). Three long-lived anticyclonic eddies in the northern south China Sea. *J. Geophys. Res.: Oceans* 116 (C05002). doi: 10.1029/2010JC006790

Nan, F., Xue, H., and Yu, F. (2015). Kuroshio intrusion into the south China Sea: A review. *Prog. Oceanogra.* 137, 314–333. doi: 10.1016/j.pocean.2014.05.012

Nitani, H. (1972). Beginning of the kuroshio. *Kuroshio Phys. Aspect Japan Current*. H. Stommel, K. Yashida, Eds. (University of Tokyo Press) 129–63.

Qiu, B., and Chen, S. (2012). Multidecadal sea level and gyre circulation variability in the northwestern tropical pacific ocean. *J. Phys. Oceanogr.* 42 (1), 193–206. doi: 10.1175/jpo-d-11-061.1

Qu, T., Kim, Y. Y., Yaremchuk, M., Tozuka, T., Ishida, A., and Yamagata, T. (2004). Can Luzon strait transport play a role in conveying the impact of ENSO to the south China Sea? *J. Climate* 17 (18), 3644–3657. doi: 10.1175/1520-0442(2004)017<3644:CLSTPA>2.0.CO;2

Qu, T., Mitsudera, H., and Yamagata, T. (2000). Intrusion of the north pacific waters into the south China Sea. *J. Geophys. Res.* 105 (C3), 6415–6424. doi: 10.1029/1999JC900323

Shen, J. Q., Fang, W. D., Li, L., Qiu, Y., Xiao, Z., Zhang, J. P., et al. (2022). Slope undercurrent in the northwestern south China Sea beneath the winter western boundary current. *Front. Mar. Sci.* 9. doi: 10.3389/fmars.2022.918077

Sheremet, V. A. (2001). Hysteresis of a western boundary current leaping across a gap. *J. Phys. Oceanogr.* 31 (5), 1247–1259. doi: 10.1175/1520-0485(2001)031<1247:HOAWBC>2.0.CO;2

Sheremet, V. A., Khan, A. A., and Kuehl, J. (2022). Multiple equilibrium states of the gulf of Mexico loop current. *Ocean Dynamics* 72 (11), 731–740. doi: 10.1007/s10236-022-01534-8

Sheremet, V. A., and Kuehl, J. (2007). Gap-leaping western boundary current in a circular tank model. *J. Phys. Oceanogr.* 37 (6), 1488–1495. doi: 10.1175/JPO3069.1

Sheu, W. J., Wu, C. R., and Oey, L. Y. (2010). Blocking and westward passage of eddies in the Luzon Strait. *Deep Sea Res. Part II: Topical Stud. Oceanogr.* 57 (19–20), 1783–1791. doi: 10.1016/j.dsr2.2010.04.004

Song, X., Yuan, D., and Li, R. (2018). Migration of mesoscale eddies across a leaping or penetrating western boundary current in the vicinity of a gap. *J. Ocean. Limnol.* 36, 2098–2109. doi: 10.1007/s00343-019-7296-9

Song, X., Yuan, D., and Wang, Z. (2019). Hysteresis of a periodic or leaking western boundary current flowing by a gap. *Acta Oceanol. Sin.* 38, 90–96. doi: 10.1007/s13131-018-1251-z

Wang, Z., and Yuan, D. (2012). Nonlinear dynamics of two western boundary currents colliding at a gap. *J. Phys. Oceanogr.* 42 (11), 2030–2040. doi: 10.1175/JPO-D-12-05.1

Wang, Z., and Yuan, D. (2014). Multiple equilibria and hysteresis of two unequal-transport western boundary currents colliding at a gap. *J. Phys. Oceanogr.* 44 (7), 1873–1885. doi: 10.1175/JPO-D-13-0234.1

Wang, Z., Yuan, D., and Hou, Y. (2010). Effect of meridional wind on gap-leaping western boundary current. *Chin. J. Oceanology Limnol.* 28 (2), 354–358. doi: 10.1007/s00343-010-9281-1

Yang, Q., Liu, H., and Lin, P. (2020). The effect of oceanic mesoscale eddies on the looping path of the kuroshio intrusion in the Luzon strait. *Sci. Rep.* 10 (1), 1–10. doi: 10.1038/s41598-020-57487-9

Yuan, D., Han, W., and Hu, D. (2006). Surface kuroshio path in the Luzon strait area derived from satellite remote sensing data. *J. Geophys. Res.* 111, C11007. doi: 10.1029/2005JC003412

Yuan, D., and Li, R. X. (2008). Dynamics of eddy-induced kuroshio variability in Luzon strait (in Chinese with English abstract). *J. Trop. Oceanogr.* 27 (4), 1–9.

Yuan, D., Song, X., Yang, Y., and Dewar, W. K. (2019). Dynamics of mesoscale eddies interacting with a western boundary current flowing by a gap. *J. Geophys. Res. Oceans* 124 (6), 4117–4132. doi: 10.1029/2019JC014949

Yuan, D., and Wang, Z. (2011). Hysteresis and dynamics of a western boundary current flowing by a gap forced by impingement of mesoscale eddies. *J. Phys. Oceanogr.* 41 (5), 878–888. doi: 10.1175/2010JPO4489.1

Zavala Sanson, L., and Van Heijst, G. J. F. (2002). Ekman effects in a rotating flow over bottom topography. *J. Fluid Mech.* 471, 239–255. doi: 10.1017/S0022112002002239

Zhong, L., Hua, L., and Luo, D. (2016). The eddy–mean flow interaction and the intrusion of western boundary current into the south China Sea–type basin in an idealized model. *J. Phys. Oceanogr.* 46 (8), 2493–2527. doi: 10.1175/JPO-D-15-0220.1